Physical Modelling in Rock Mechanics and Rock Engineering

Rock Mechanics and Rock Engineering
https://doi.org/10.1007/s00603-024-04106-y

ORIGINAL PAPER

Physical Modelling in Rock Mechanics and Rock Engineering

Herbert Einstein[1]

Received: 3 May 2024 / Accepted: 31 July 2024

Abstract

The paper presented at the International Congress and this extended version are intended to pay homage to Professor Leopold Müller who was a leading developer and user of physical models. This will be done by first reviewing physical models of stone-built artificial structures from ancient times till now being used to investigate the flow of forces and the effect of material properties. The same issues affect rock mechanics and engineering. Consequently, physical Querymodels of fundamental material behavior, geologic mechanisms, and especially jointed rock will then be described. On this basis complex models of geologic processes and of structures on and in rock masses will be discussed. Finally, critical aspects, namely, the issues of scaling and of possible obsolescence because of powerful simulation models, will be addressed leading to the outlook where physical models can and should be used.

Highlights

- Physical Models play a major role in rock mechanics and rock engineering.
- This paper reviews the history of material models, geologic models and combined geologic/structural models.
- Physical models are compared to simulation models.

Keywords Physical models of geology of structures in and on rock and processes in rock · History of physical modeling · Comparison physica/simulation models

1 Introduction

This paper intends to pay homage to Professor Leopold Müller who was a leading developer and user of physical models to solve fundamental rock mechanics problems and complex engineering cases. Professor Müller not only used Physical Models extensively but also wrote a classic paper (Müller 1980), in which he discussed other types of models and addressed the skepticism with which physical models were looked at. Today we face a similar situation in that the use of physical models is questioned in comparison to the possibilities of powerful computer-based simulations. There is also the issue that physical models can be differently defined, which will be addressed by providing a variety of examples—not all-encompassing but reasonably representative.

I intend to start by reviewing the history of models representing stone-built structures in the antiquity and later, worldwide. The objective of these structural model tests was to determine the flow of forces and their effect on structural performance quite analogous to the model investigations of rock masses, the main topic of this paper.

Interestingly, when geology moved from descriptive to mechanics-based approaches in the nineteenth century this was accompanied by physical models. The logical next step was then to consider the interaction of the rock mass and engineering structures be they dams, rock cuts, or underground openings.

Finally, to bring physical modeling into the context of present-day engineering and science this paper will compare the principles and use of physical models with those of simulation models. As will be shown both can and should be

✉ Herbert Einstein
einstein@mit.edu

[1] Massachusetts Institute of Technology, Cambridge, MA, USA

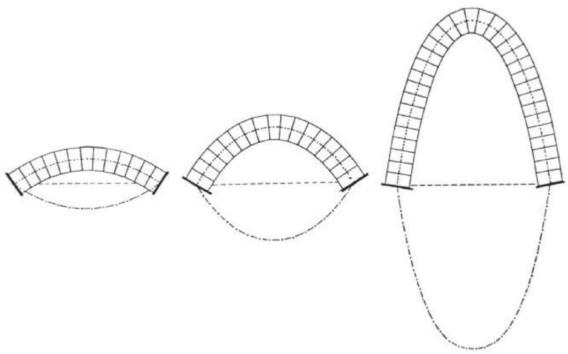

Fig. 1 Hooke's second law (Addis 2021)

used and can complement each other and serve to validate each other.

It is important, and as will be seen in the body of the paper, to know that physical modeling has been discussed quite widely. This paper is based on the systematic approach described above but what is discussed can only be limited.

2 Physical Models of Artificial Structures

Human beings have used physical models for structures they built initially mostly for visualization purposes but soon also for mechanical functionality. This will be briefly reviewed with the information coming from the two sources: Addis (2021) and Mindrup (2019).

In Egypt 2000–1600 BC it evidently was quite usual to build funerary models before creating them in reality, a process which one can call visualization or architectural modeling. Particularly interesting regarding architecture are miniature models of columns. Markers on these (600–400 BC) models indicate that the models were used to scale the geometry up (Mindrup 2019).

According to Mindrup (2019) the ancient Greeks did not use scaled models, but full-scale exemplars (prototypes) so-called Paradeigmata. This was evidently also done for the famous Eupalinos Aqueduct Tunnel (Kienast 2005) in Samos (Sixth century BC) for which a five-meter-long section marked with the word Paradeigma indicates that it was not only used as a trial section for the Eupalinos tunnel but possibly for others.

Not related to structural modelling but because of scaling, according to Addis (2021), Philon and Heron and others reported on the use of models to design and build catapults. Not only were they used to develop optimal mechanisms but also to scale the projectiles.

Probably no better example of the use of models for design is the Dome of Sta. Maria del Fiore in Florence. In the fourteenth century the Opera del Duomo (the agency in charge of rebuilding the dome) initiated a design competition with models and drawings for the cupola of the dome. Neri di Fioravanti proposed a cupola internally supported by chains, while Talenti and Giovanni di Lapo Ghitini proposed a "gothic " design with external buttresses. Mindrup (2019) describes in detail the roles of models in this competition; however, none of the proposals was realized. Realization only happened with Brunellesci's design who in 1418 proposed a dome design without centering (scaffolding). Brunellesci's design was again chosen based on a competition with models. Brunellesci's model was *"a large 1:12 double-shell masonry model of the cupola—more than 2 m wide and 3.5 m tall"* (Mindrup 2019).

These models were mentioned because they show what is also crucial in rock modeling: The flow and magnitude of forces has to be such that the tensile stresses are below the critical ones for the brittle material, and they have to be such that a blocky structure does not become unstable.

These problems are also addressed by modern models, which are in essence based on the philosophy of Hooke's second law: "As hangs the flexible line, so but inverted will stand the rigid arch" (Fig. 1). So, if one inverts a catenary, which is entirely in tension, the resulting shape will be entirely in compression.

Isler (1961) extends this to three dimensions with his "hanging cloth reversed" (Fig. 2) method. As Isler(1961) and Chilton (2021) in Addis (2021) state the problem and solution by physical modeling is not that simple: Compression may cause buckling at the boundaries and material selection for the models is very involved.

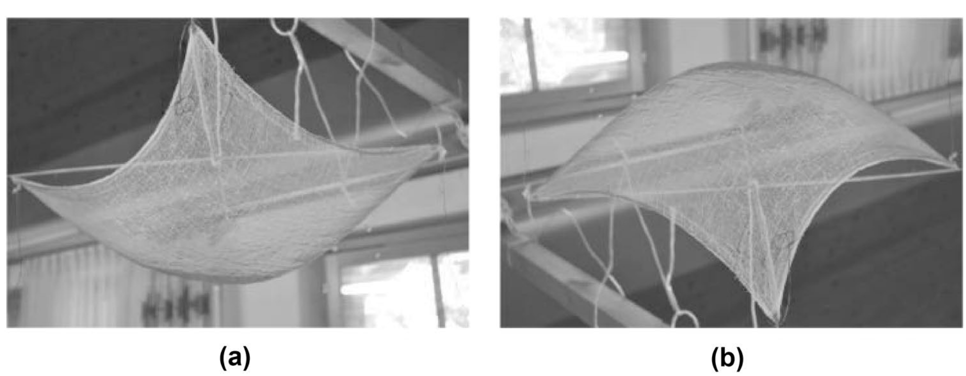

Fig. 2 **a** One of many hanging cloth models made by Isler; **b** The same model shown inverted for use as a compression structure (Image: John Chilton). Ref: Chilton in Addis (2021)

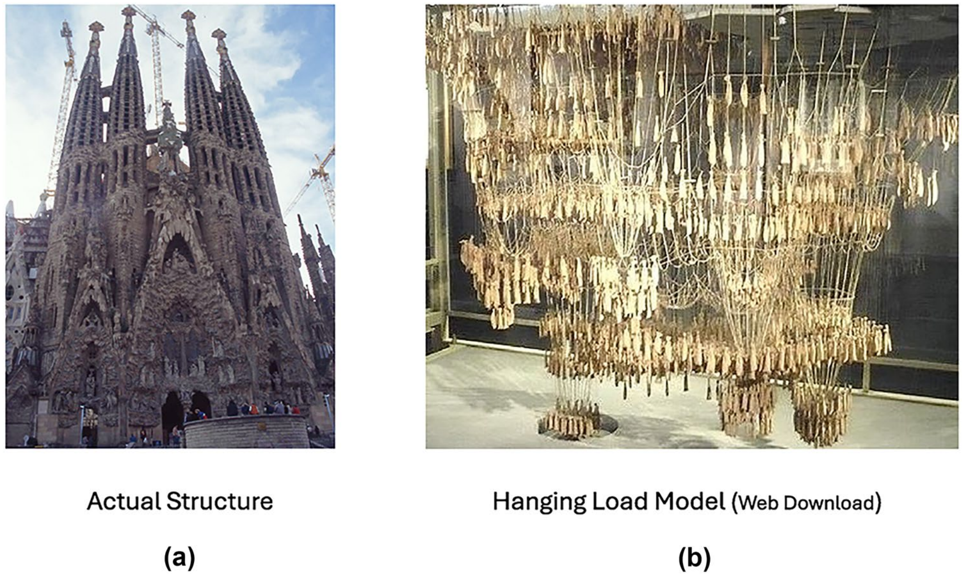

Fig. 3 Sagrada Familia by Gaudi. **a** Built structure (Photo H. Einstein); **b** Reverse hanging model (Web Download)

The extreme application of Hooke's second law is what Gaudi did, e.g., with the Sagrada Familia Fig. 3.

The review of models for artificial structures showed that the model needs to consider the material and the geometry, and these need to be properly scaled. As will be shown now this is exactly what needs to be done with physical models for rock mechanics and rock engineering.

3 Material and Geologic Models

3.1 Basic Material Models

To start this section the discussion (dialogo secondo) by Galilei (1638) on bending (Fig. 4) is used. Figure 4 shows not the picture of a physical model but of a conceptual one. It is used because it shows two aspects (among others) of

114 DIALOGO SECONDO

ſin quì dichiarate, non ſarà difficile l'intender la ragione, onde auuenga, che vn Priſma, ò Cilindro ſolido di vetro, acciaio, legno, ò altra materia frangibile, che ſoſpeſo per lungo ſoſterrà graviſſimo peſo, che gli ſia attaccato, mà in trauerſo (come poco fà diceuamo) da minor peſo aſſai potrà tal' volta eſſere ſpezzato, ſecondo che la ſua lunghezza eccederà la ſua groſſezza. Imperò che figuriamoci il Priſma ſolido AB, CD fitto in vn muro dalla parte AB, e nell' altra eſtremità s'intenda la forza del Peſo E, (intendendo ſempre il muro eſſer eretto all' Orizonte, & il Priſma, ò Cilindro fitto nel muro ad angoli retti) è manifeſto che douendoſi ſpezzare ſi romperà nel luogo B, doue il taglio del muro ſerue per ſoſtegno, e la BC per la parte della Leua, doue ſi pone la forza, e la groſſezza del ſolido BA e l'altra parte della Leua, nella quale è poſta la reſiſtenza, che conſiſte nello ſtaccamento, che s' hà da fare della parte del ſolido BD, che è fuor del muro, da quella che è dentro; e per le coſe dichiarate il momento della forza poſta in C al momento della reſiſtenza che ſtà nella

Prop. I.

Fig. 4 Galileo's Beam/cantilever theory (from Linda Hall Library, Kansas City MO)

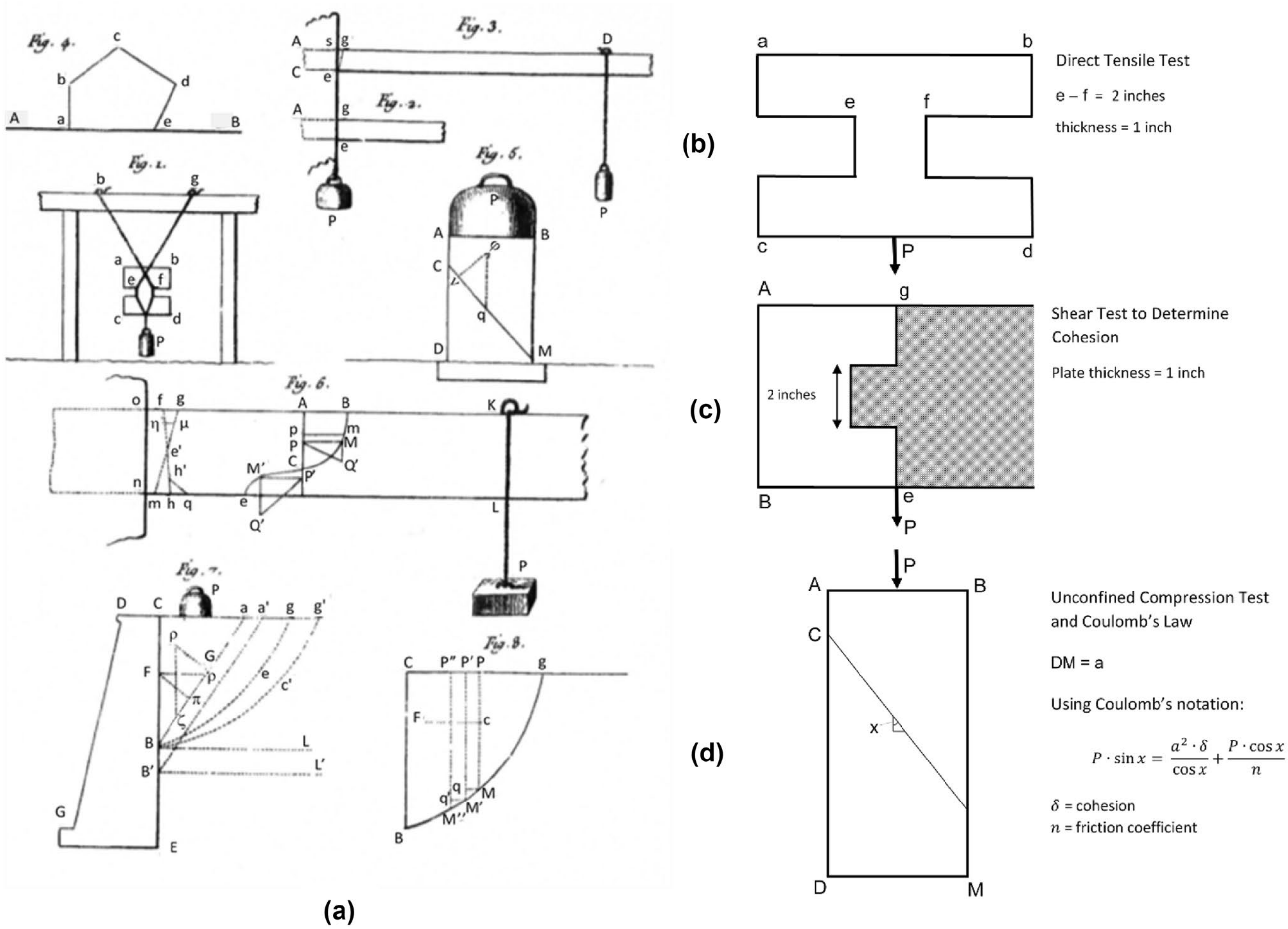

Fig. 5 From Coulomb (1776) (**a**) Plate I in Coulomb (1776); (**b**) Schematic of Fig. 1 in Plate I Coulomb (1776); (**c**) Schematic of Fig. 2 in Plate I Coulomb (1776); (**d**) Schematic of Fig. 5 in Plate I Coulomb (1776)

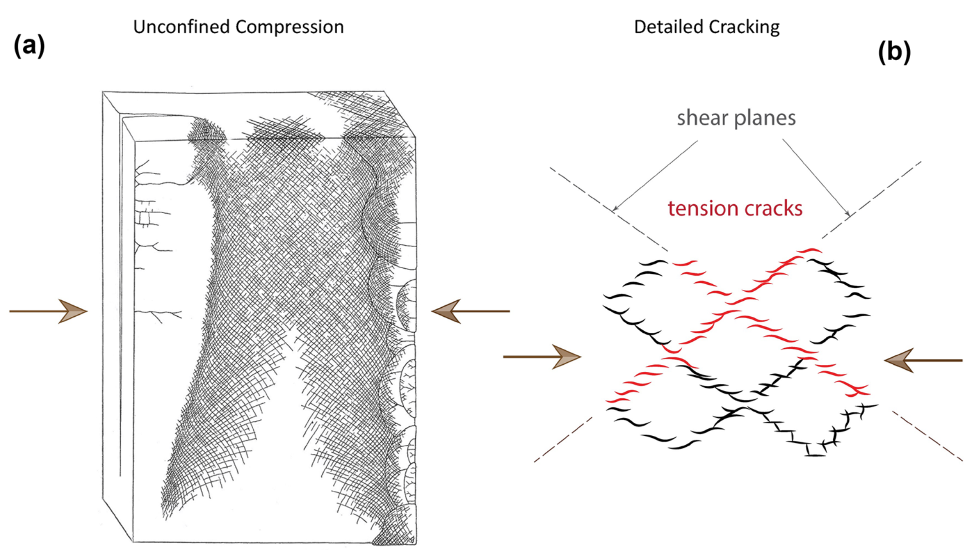

Fig. 6 Test on blocks of paraffin and resin at 0° F (Shelton 1912). (**a**) Overall observations; (**b**) Details

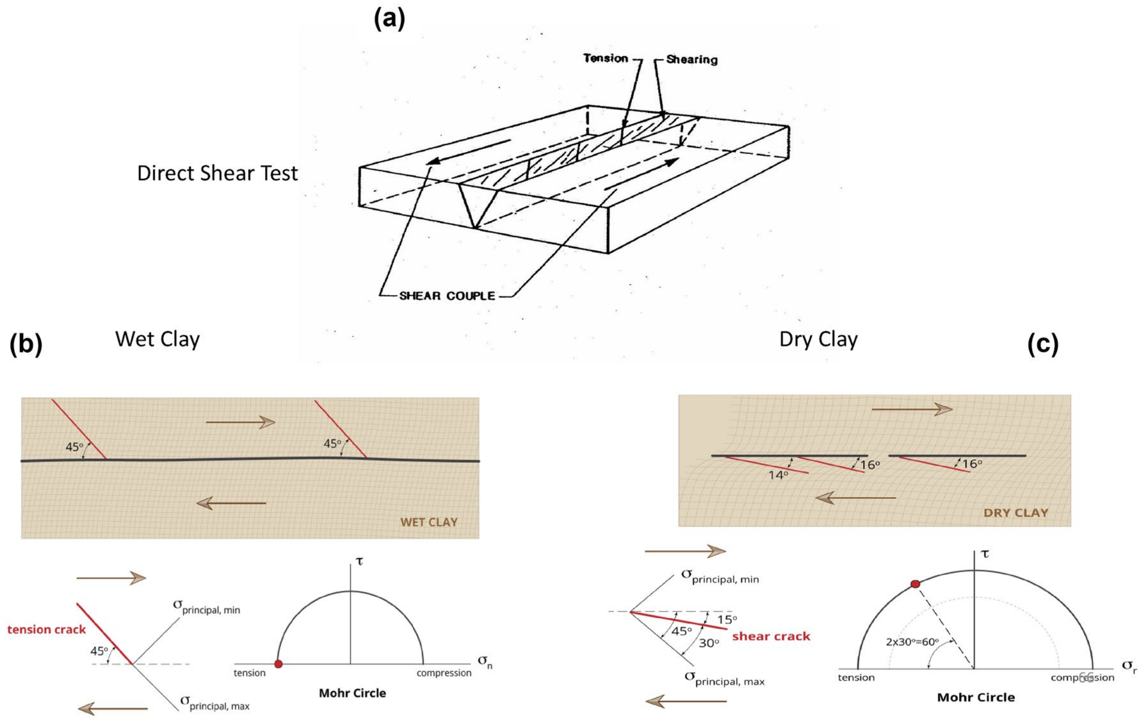

Fig. 7 Direct shear tests on clay (Riedel 1929). (**a**) Schematic of direct shear test; (**b**) Fracture geometry and Mohr circle for wet (weak) clay; (**c**) Fracture geometry and Mohr circle for dry (strong) clay

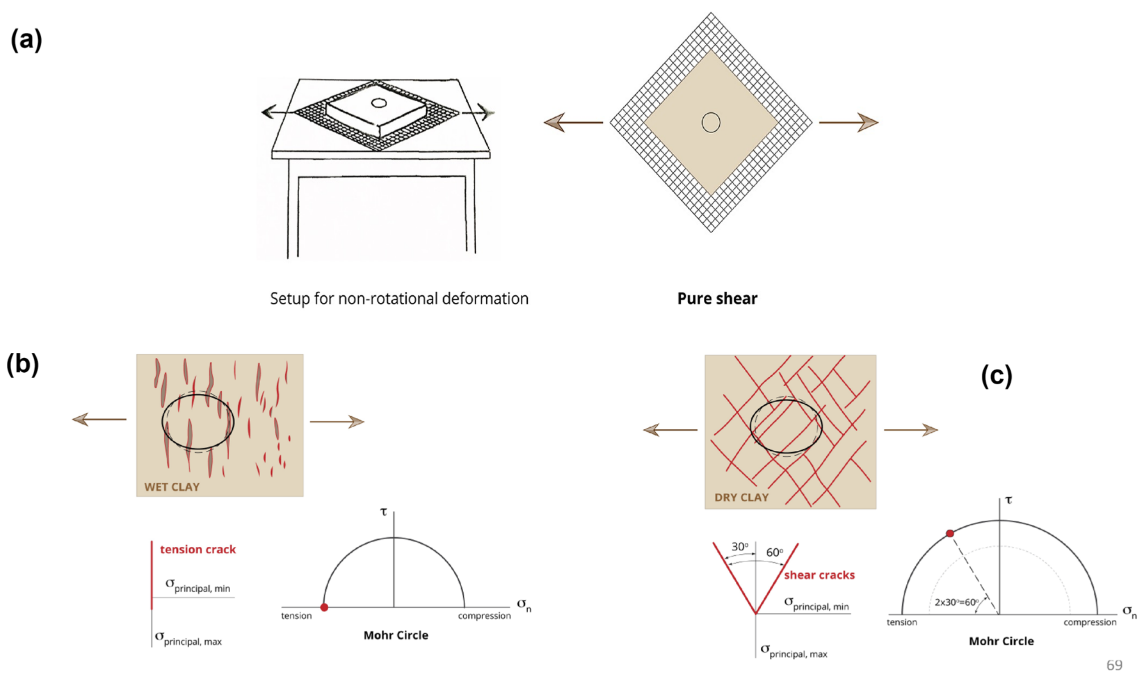

Fig. 8 Pure shear tests on clay (Cloos 1955). **a** Schematic of pure shear test; (**b**) Fracture geometry and Mohr circle for wet (weak) clay; (**c**) Fracture geometry and Mohr circle for dry (strong) clay

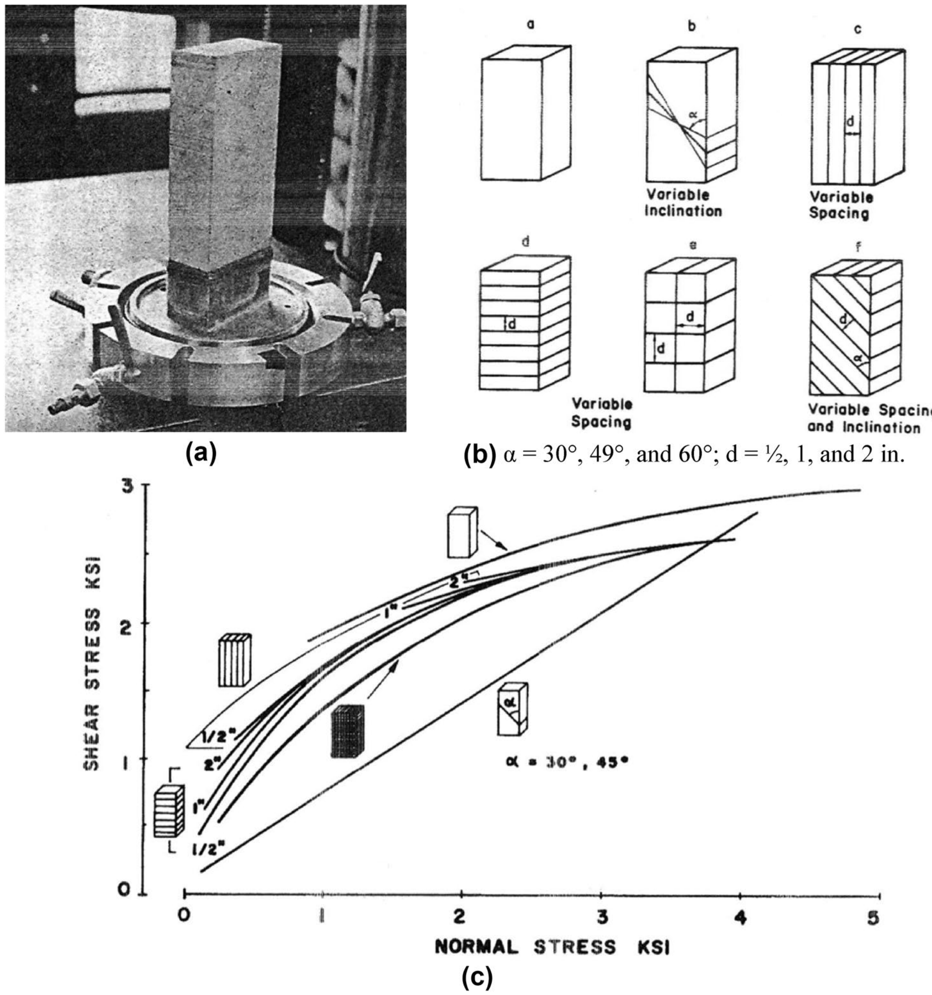

Fig. 9 Triaxial tests on jointed gypsum model rock (from Einstein et al. 1969). (**a**) Triaxial test setup; (**b**) Different joint geometries; (**c**) Mohr envelopes for the different joint geometries

Fig. 10 Direct shear tests on jointed model rock (Ladanyi and Archambault 1969). The Model Rock consists of ½ × ½ × 2 ½ inch concrete rods

Galilei's interpretations: the correct one is related to scaling: multiplying (e.g., doubling) the dimensions does not increase the loading capacity by the same factor. The incorrect one is the assumption that the distribution of tensile stresses is uniform at section A–B while in reality it is triangular. If a physical model test had been run this mistake might have been discovered.

Coulomb (1776) on the other hand uses detailed experiments (Fig. 5a) to not only illustrate but also measure cohesion. As a matter of fact, he measured both tensile strength and cohesion of Bordeaux limestone (Pierre de Bordeaux—calcaire à Astéries). Figure 5b shows the tensile strength measurement on a one-foot square 1-inch-thick slab with a two-inch neck. The resulting failure force was 430 pounds and thus the tensile strength 215 pounds/square inch. Determination of cohesion with a direct shear test was done by having a mortise and tenon along the plane g–e in Fig. 5 c and applying force P by slinging a rope in plane geP. The tenon was 2 × 1 inches, i.e., the same cross-sectional area as in the direct tension tests. The resulting shear load at failure was 440 pounds and cohesion 220 pounds/square inch, i.e., higher than the tensile strength. Coulomb did mention

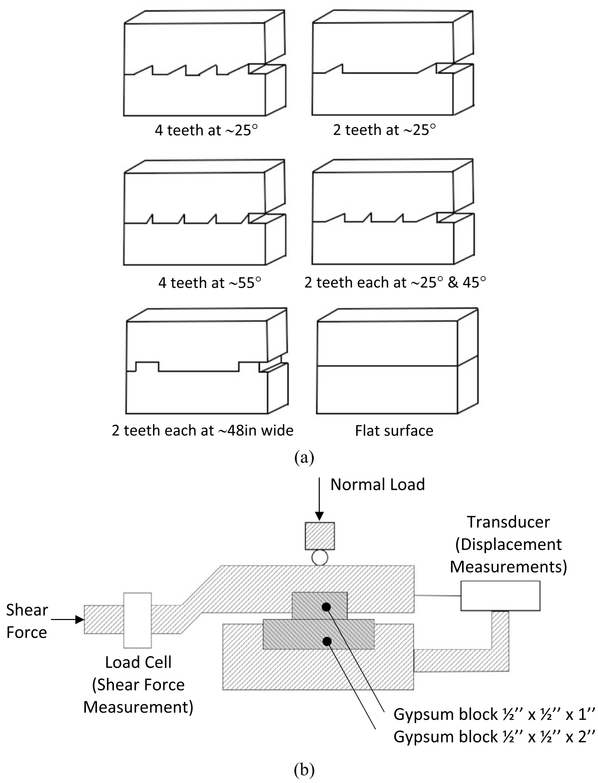

Fig. 11 Direct shear tests on joints. (**a**) Geometries tested (Patton 1966); (**b**) Schematic of test equipment (Einstein et al 1969)

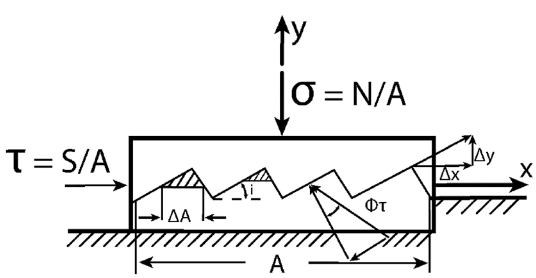

Fig. 12 Schematic of Ladanyi and Archambault (1969) model

this fact but did not further pursue this since the difference was small and varied (note and thinking of Mohr diagrams: equality of cohesion and tensile resistance occurs only with a parabolic envelope (see Hoek, 1968), while a straight-line envelope can lead to differences in cohesion and tension depending on the assumed friction angle). Very importantly, Coulomb did multiple tests using not only limestone but also artificial materials (bricks and mortars). Equally important, he mentions that one cannot generalize the results since they differ for different materials. Interestingly, Coulomb mentioned friction only marginally by citing Amontons, and he developed the "Coulomb law" theoretically in the context of

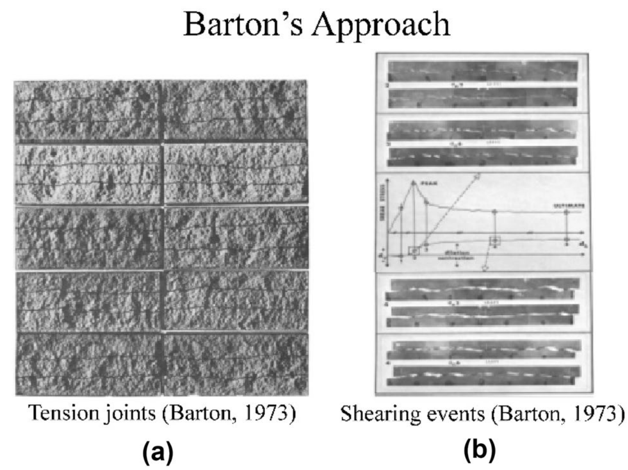

Fig. 13 Barton's (1970, 1971, 1973) model tests (**a**) surfaces of different tension joints, (**b**) analog direct shearing test along a 2-D profile: plastic strips representing a joint with two rough surfaces are displaced—"sheared"—relative to each other

an unconfined compression test (Fig. 5d) and this in terms of forces. He did not run a test to verify the law.

Mohr (1906) did not perform tests by himself but used tests run by others to confirm what he proposed theoretically: the sliplines bisect the angle between the major and minor principal stresses in a tension test, and the angle between the major principal stress and the failure surface in a compression test becomes smaller with increasing material strength, i.e., the failure envelope is curved.

3.2 Geologic Models in the 19th and Early 20th Century

While Coulomb and Mohr used the physical models to prove their theories, Shelton (1912), Riedel (1929), Cloos (1930), and Cloos (1955) used their model tests to explain fracture patterns observed in nature. Sheldon used paraffin–resin models at 0° F to explain joint geometries she had observed in nature. The experiments showed the patterns documented in Fig. 6a where uniaxial compression was applied along the horizontal axis resulting in new fractures inclined at 45° to the force direction implying zero frictional resistance. Most interesting is the observation shown in Fig. 6b with classic wing cracks aligned along the major principal stress direction.

The Riedel (1929) and Cloos (1955) experiments show both the influence of the shear mechanism, namely, direct shear versus pure shear, together with the effect of material strength, namely, wet versus dry clay (note that Cloos achieved wet clay by sprinkling water over the clay surface) (see Figs. 7 and 8).

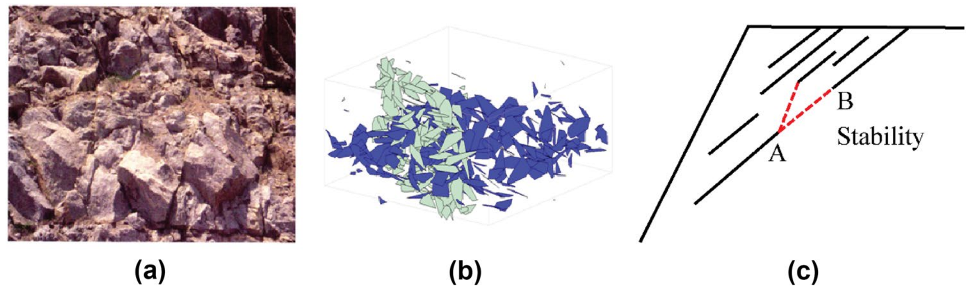

Fig. 14 Fracture system geometry and failure. (**a**) Outcrop with fracture system; (**b**) Discrete fracture geometry (DFN) model Geofrac representing complex fracture system; (**c**) Complex failure mechanism through intact rock bridges

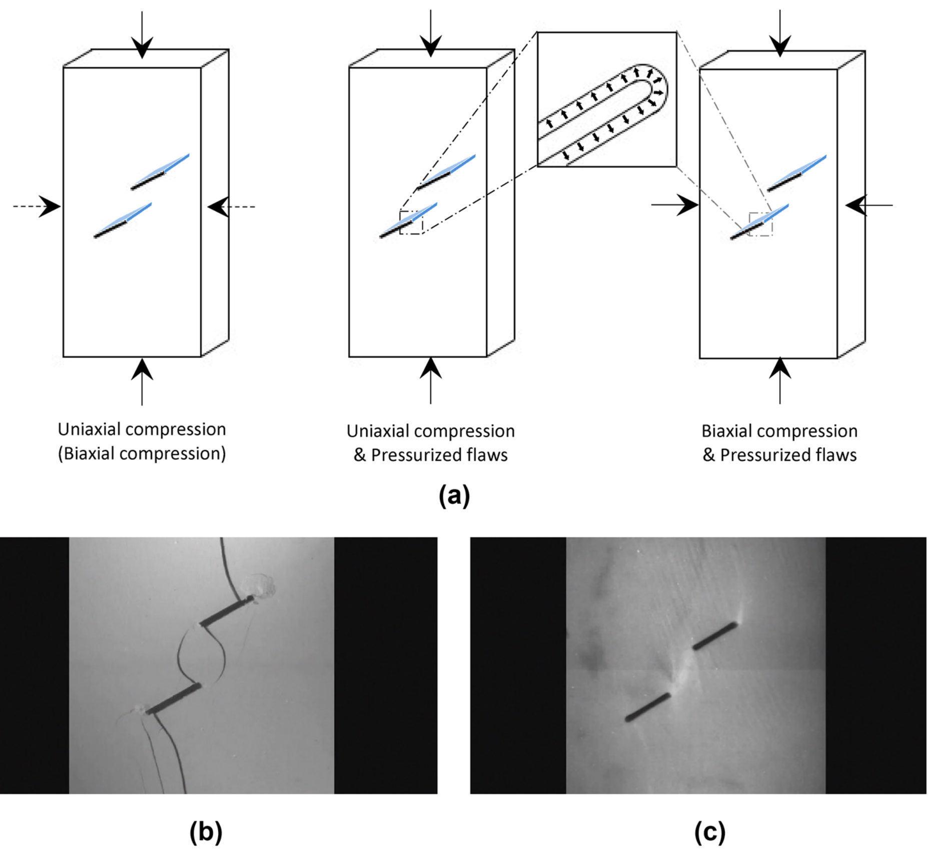

Fig. 15 Physical model testing addressing the "persistence problem". (**a**) Prismatic physical models under different stress conditions, different joint geometries, different materials, and different flaw geometries. The flaws are rectangular and go through the prismatic specimen. (**b**) Test result of a uniaxial compression test on gypsum showing classic tensile "wing" fractures. (**c**) Test result of a uniaxial compression test on marble showing shear failure. The uniaxial load in **b** and **c** is applied in the vertical direction

3.3 Jointed Rock Models

The next step was to investigate the behavior of jointed rock, i.e., strength and deformability of a jointed rock mass. Figure 9 presents aspects of the work by Einstein et al. (1969). Figure 9a shows the relatively complex triaxial equipment that was used to run tests on rock models consisting of Gypsum blocks representing a rock mass with different joint (fracture) spacings and orientations (Figs. 9b). The complexity was caused by the necessity of having prismatic specimens causing challenges regarding sealing. Very interesting are the results potted with the Mohr diagrams of Fig. 9c. The results indicate decreasing strengths with increasing numbers of preexisting joints being intersected by the failure surface (the stress–strain plots show analogous behavior – see EE Einstein et al. 1969 Einstein and Hirschfeld 1973)

These results are emphasized here because they then led to the physical model research on non-persistent fractures (see, e.g., Reyes and Einstein 1991; Bobet and Einstein 1998) discussed later in this paper. It is important to note that around the same time others (Hayashi 1966; Rosengren and Jaeger 1968; Rosenblad 1969; Ladanyi and Archambault 1969; Brown and Trollope 1970) conducted analogous tests on jointed rock models. The work by Brown and Trollope (1970) is interesting because it eventually led to the Hoek and Brown criterion (Hoek et al. 2002).

Figure 10 from Ladanyi's and Archambault's (1969) paper represents a transition between the behavior of an

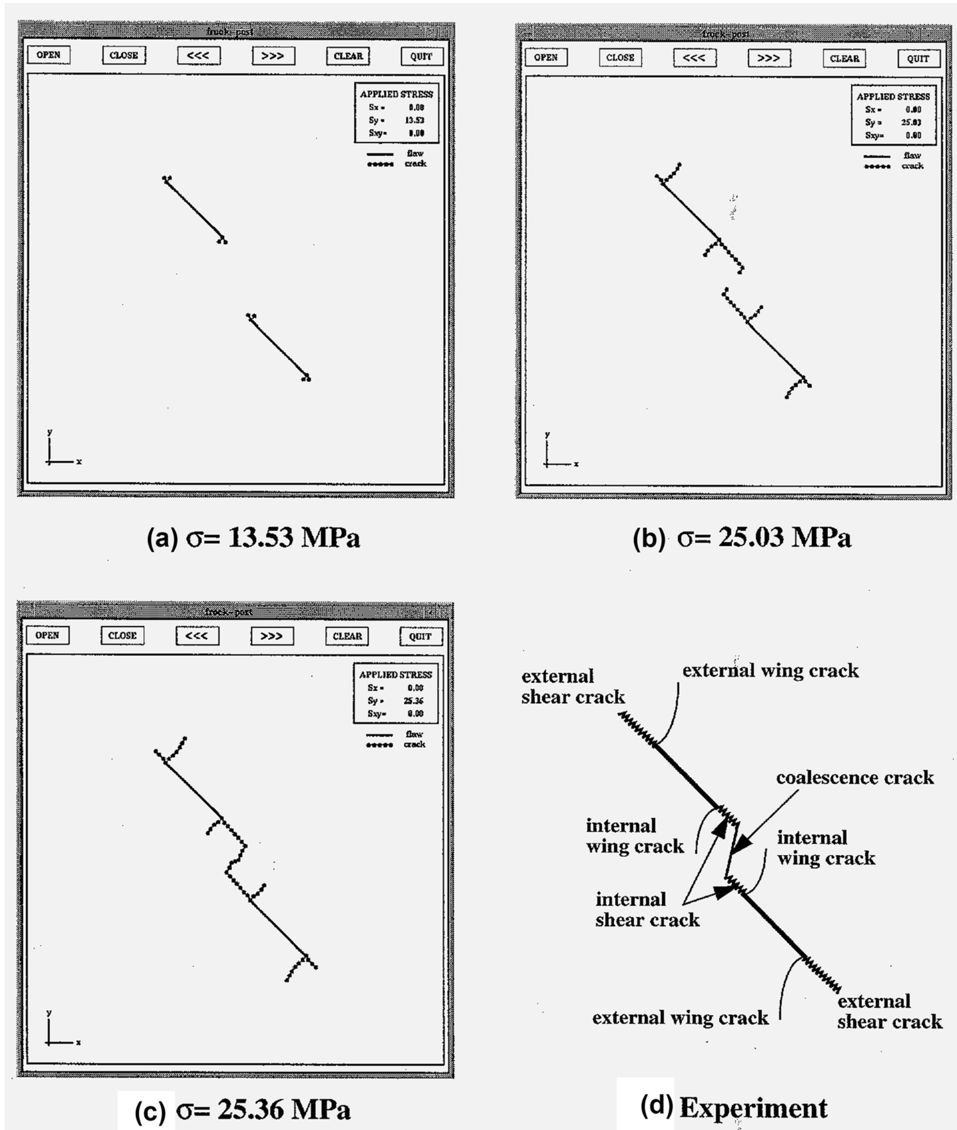

Fig. 16 Comparison between numerical prediction and experiment for a 45-a-2a open flaw geometry in uniaxial compression (Bobet and Einstein 1998)

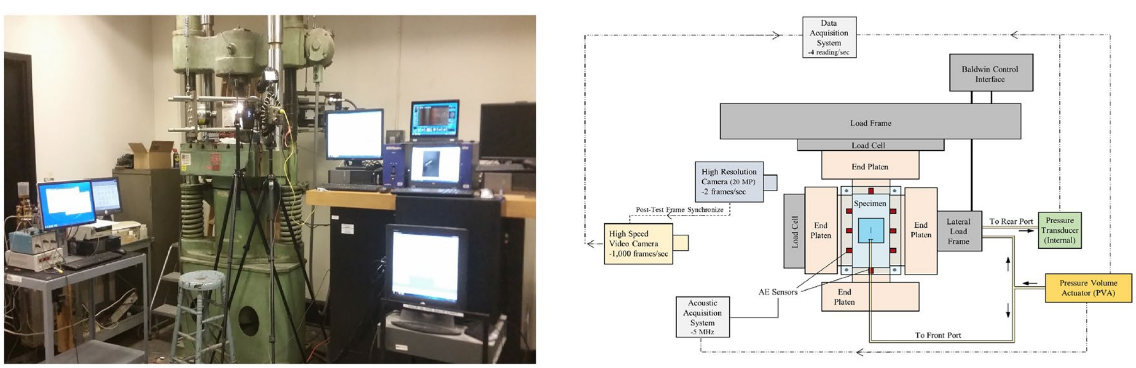

(a) (b)

Fig. 17 Loading and recording equipment used to conduct physical model tests on the persistence problem and hydraulic fracturing. (**a**) Photo, (**b**) Schematic

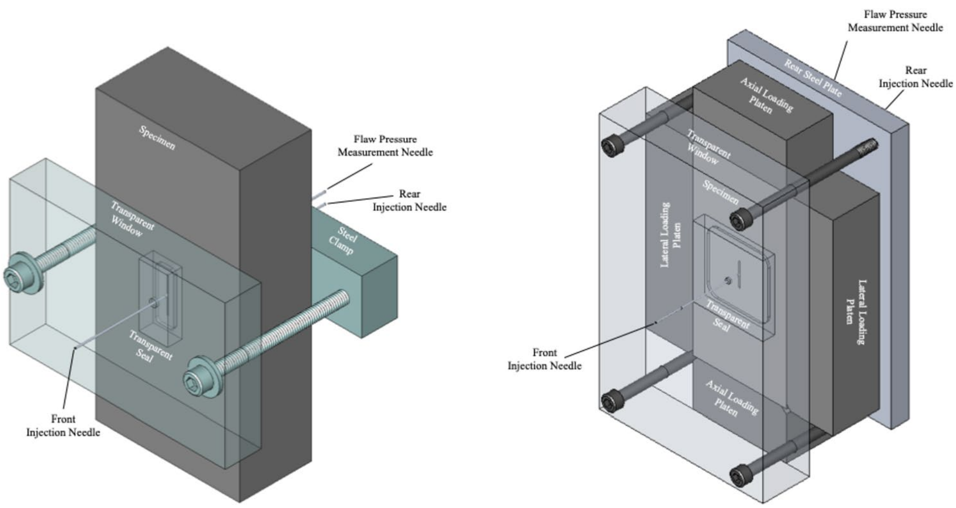

Fig. 18 Equipment for application and visualization of hydraulic fracturing. (**a**) In uniaxial test on 2 × 3 × 6″ specimen; (**b**) In bi-axial (quasi-triaxial) test on 1 × 2 × 4″ specimen

individual joint discussed below and the behavior of a rock mass.

To completely represent the behavior of a jointed rock mass it is necessary to model the behavior of the individual joint, specifically the effect of joint roughness on shearing resistance. Early work in this direction is by Patton (1966) and Goldstein et al. (1966). Patton (1966) qualitatively characterized the effect of joints on the stability of rock slopes and also conducted model tests on the effect of asperities on direct shear resistance (Fig. 11a). Similar tests were run at that time by the Hirschfeld group at MIT (Fig. 11b) as reported, e.g., in Einstein et al 1969. Patton's work also included development of a theoretical model representing shearing-off and riding-over asperities. Note in this context that the shearing mechanisms of individual joints is more complex as discussed by Nelson (1977).

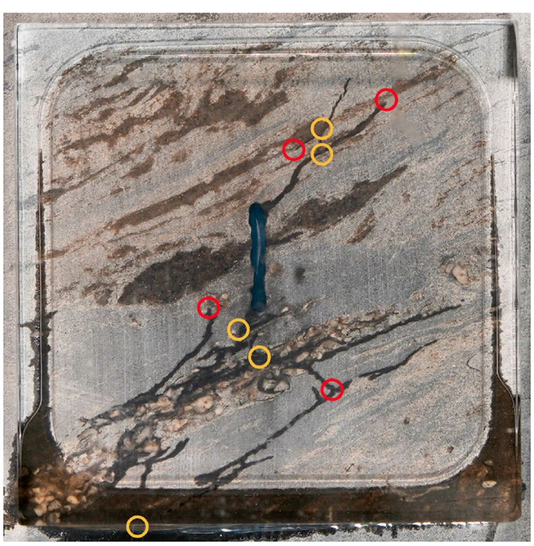

Fig. 19 Visualization of hydraulic fracturing on Opalinus clayshale (red circles: propagating fracture stops; yellow circles—propagating fracture stops temporarily; the square seal on the face of the specimen is 1.5″ × 1.5″)

The shearing mechanism of an individual joint, i.e., the above-mentioned combination of shearing-off of asperities affected by "intact rock" resistance and the "riding-over" of asperities affected by sliding resistance, was included in the testing and theoretical modeling work by Ladanyi and Archambault (1969) as schematically shown in Fig. 12.

Barton in his Doctoral Thesis (Barton 1970) did also work along these lines with extensive experimental modeling. Specifically, joints in a model material were created through indirect tension (guillotine) and then tested in shear. In addition, profiles along the black lines in Fig. 13a were transformed into 2-d plastic-sheet profiles shown in Fig. 13b. All this was then combined in the shear force–displacement diagram also shown in Fig. 13b. With this information Barton (1973) then formulated his joint shearing resistance expression, which also include the joint roughness coefficient JRC. Further developments, e.g., Barton and Bandis (1982), Barton and Choubey (1977) also involving laboratory experiments led to consideration of size effects.

From this point on the physical modeling went into two directions.

- Details of the fundamental fracturing mechanisms (see below).
- Modeling of large-scale mechanisms such as slope failures and interaction with structures such as dams and tunnels (the latter will be dealt with in Sect. 4).

For the former the changing Mohr envelopes of Fig. 9 provide an idea: analysis showed that if the physical failure surface crossed more joints this led to lower Mohr envelopes, in essence indicating that these crossing points were possible fracture initiation points. In addition, parallel theoretical

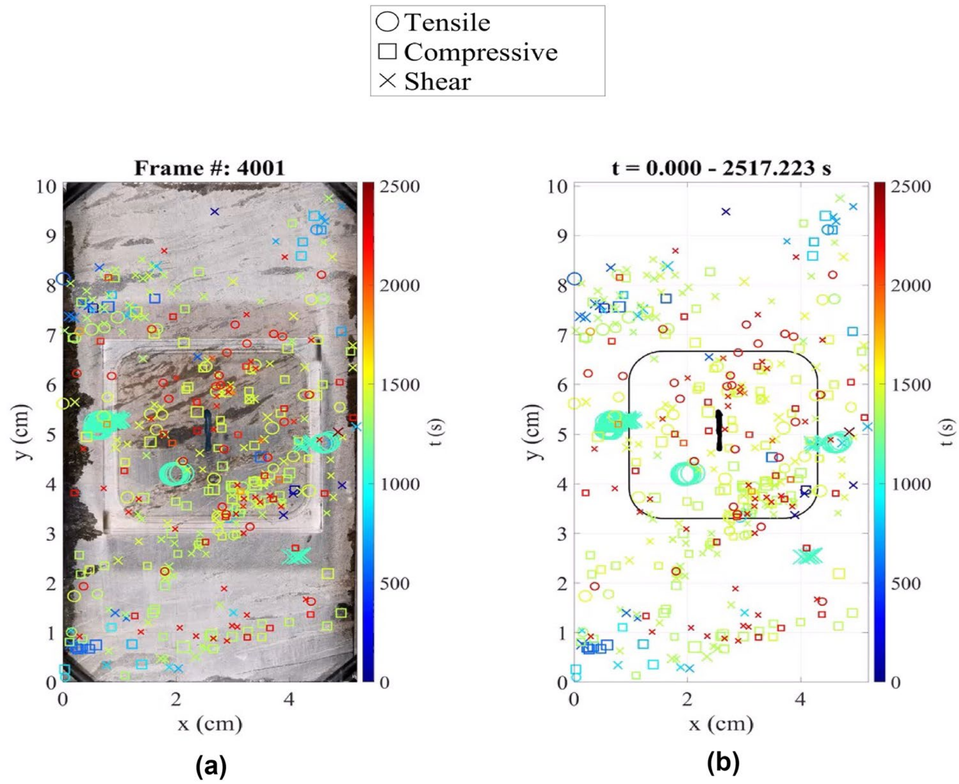

Fig. 20 Same test as Fig. 19. (**a**) Visualization of fracturing with records of acoustic emission events superimposed; (**b**) Acoustic emission events (colors indicate timing, size indicates magnitude, symbols: x double couple–circle expansion/tensile–square collapse/compressive)

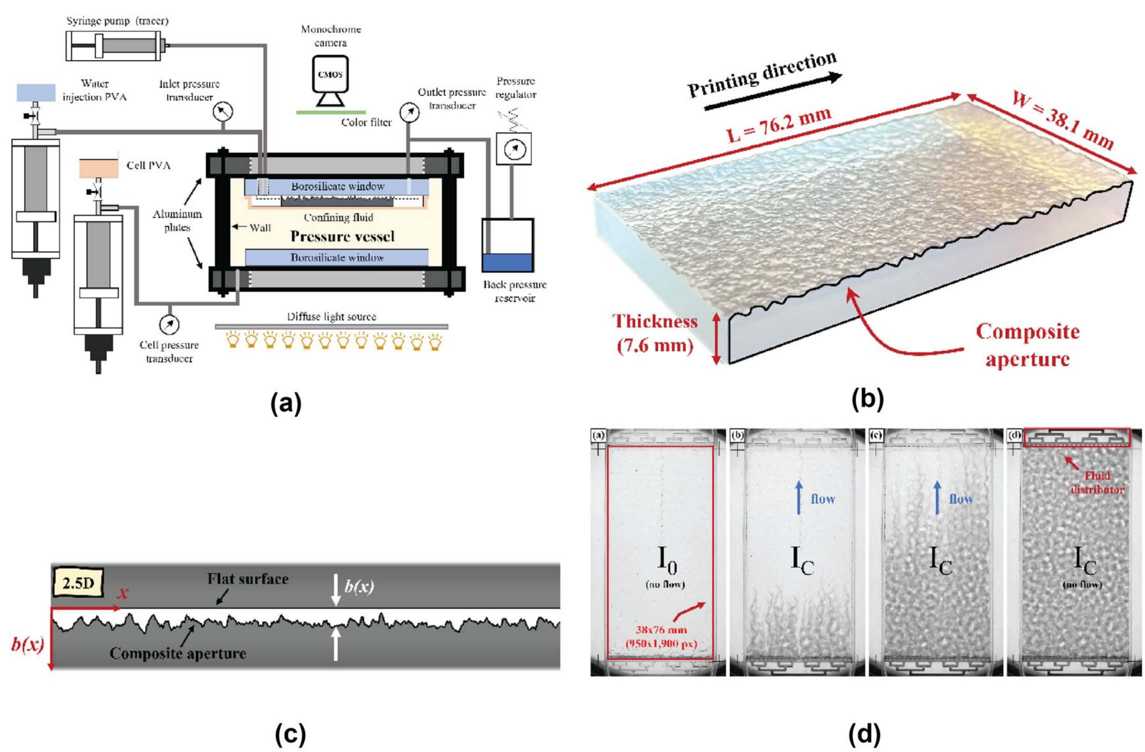

Fig. 21 Flow experiments on individual rough fracture using a Hele Shaw cell. (**a**) Schematic cross-section; (**b**) transparent analog; (**c**) Schematic cross-section of rough fracture; (**d**) Deformation of contacts and flow under increasing pressure

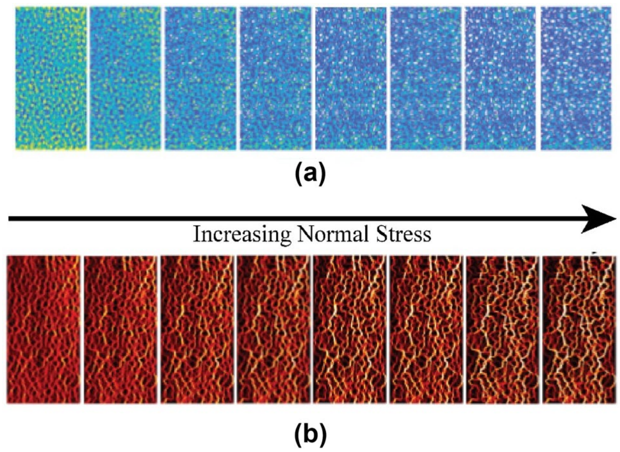

Fig. 22 Results of flow experiments on individual rough fracture using a Hele Shaw cell under increasing normal stress. (**a**) Fracture asperities in contact—white indicates contact area; (**b**) Flow channeling

investigations on the stochastic nature of joints (see Fig. 14a and, e.g., Baecher et al. (1977), Call et al. (1976), Dershowitz (1984), Dershowitz and Einstein (1988)) eventually led to DFN's (Fig. 14b) and influenced the analytical modeling of failure of jointed rock masses: Einstein et al.(1983) and Einstein et al.(1980) showed that the eventual failure of intact rock bridges can be complex combinations of shear and tensile failure (Figs. 14c). This indicated that it was necessary to physically investigate this rock bridge failure problem also called the "persistence problem."

Following numerical model work by Chan et al. (1990) that led to the development of FROCK (Fractured ROCK), Reyes and Einstein(1991) and Bobet and Einstein (1998) studied fracture interaction with physical models. The physical model tests with different materials and geometries, and different applied stresses (Fig. 15a) showed different interaction mechanisms (Fig. 15b and c). The research by Bobet and Einstein (1998) started an extensive series of tests initially using the same model material (gypsum), in which

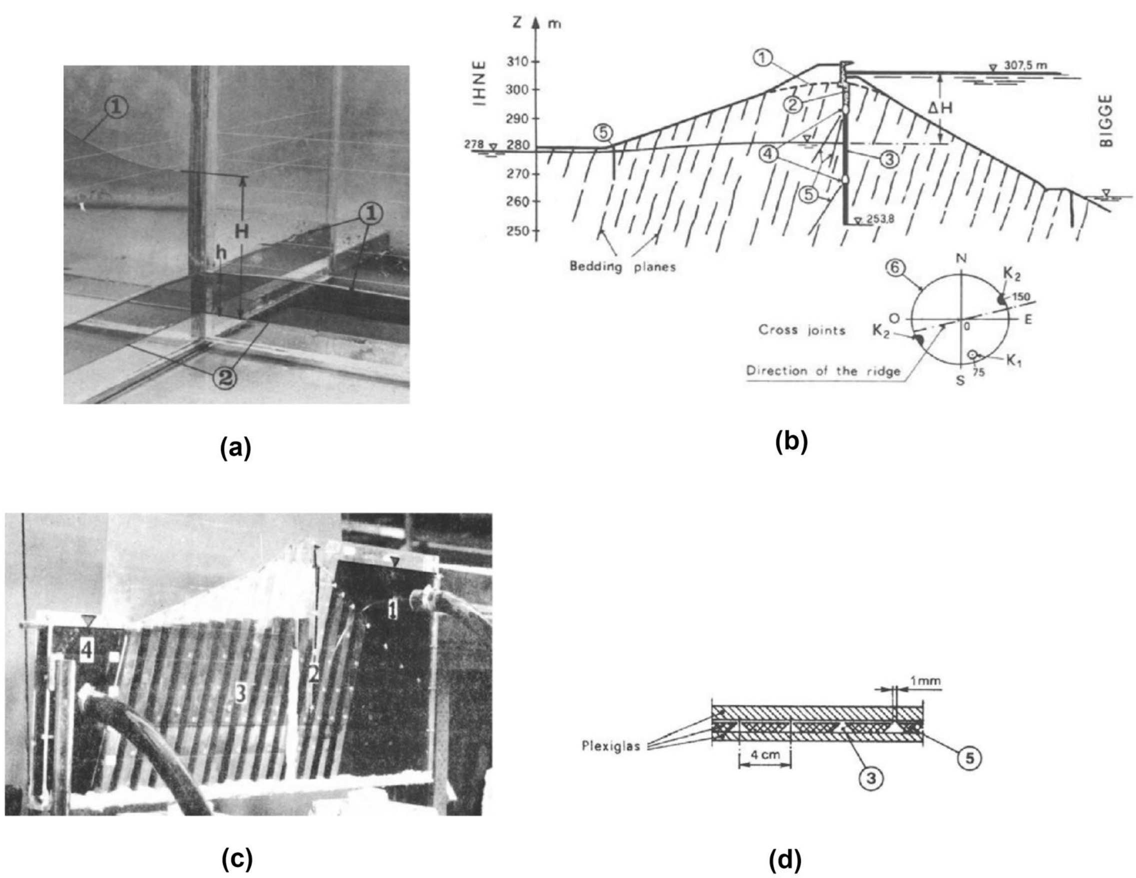

Fig. 23 Physical model for flow through a jointed rock mass (Louis 1972). (**a**) Experimental study of the flows in the neighborhood of the intersection of two fractures: (1) Free surface (2) Impermeable boundary where H and h are piezometric heights; (**b**) Cross-section of the ridge "Kraghammer Sattel": (1) Natural profile (2) Concrete piling (3) Grout curtain (4) Controlling galleries (5) Piezometers and drainage (6) Main fractures in zone 1; (**c**) Hydraulic model for study of flows in zone I of Kraghammer Sattel: (1) Reservoir at 307.5 m level (2) Grout curtain (3) Simulation of the bedding (4) Downstream level 278 m (5) Simulation of cross-joints K2; (**d**) Joint details

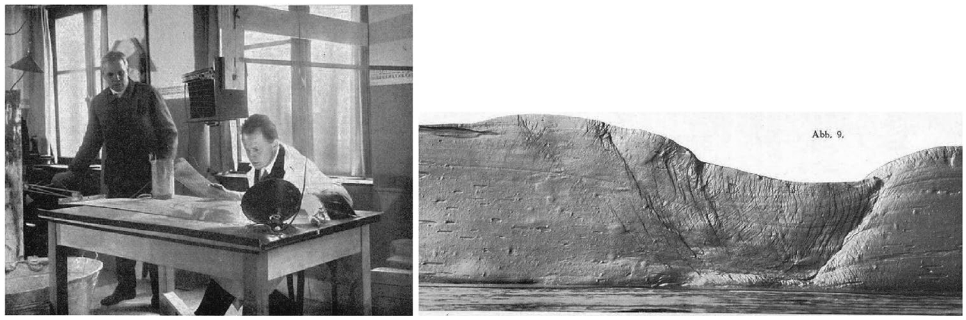

(a) (b)

Fig. 24 Conceptual physical model of H. Cloos (1930). (**a**) Table with clay sheet under which a metal sheet is pulled to deform the clay sheet; (**b**) Graben produced with the modeling process of (**a**).Vertical height of Graben approx. 10 cm

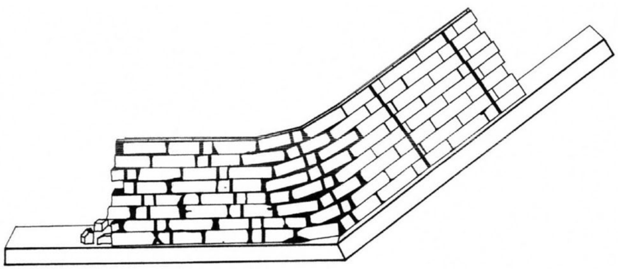

Fig. 25 Physical Model of Mount Toc Slide Conducted by L. Müller (from Fumagalli 1973)

the geometry of the preexisting fractures was varied and compared to the numerical model (FROCK) (Fig. 16).

Given the practical and research interest in hydraulic fracturing, testing was extended by adding the effect of fluid pressure. At MIT these tests were mostly on natural rock and not on model material with the equipment shown in Figs. 17 and 18. Most important in the experiments conducted with this equipment is the possibility to simultaneously observe and record fracture propagation both visually and with acoustic emission (Figs. 19 and 20).

Physical models can not only be used to conduct experiments on fracturing but on flow and, specifically, fracture-flow. The following will therefore deal with modeling fluid–rock interaction first of the individual joint and then the jointed rock mass. Individual joint models mostly concentrate on the effect of irregular joint surfaces on fluid flow. Many use natural rocks with natural or artificially cut fractures/joints (see, e.g., Iwano and Einstein 1995). Using such non-transparent materials causes problems in that the surfaces and the flow through fractures cannot be directly observed and have to be inferred. More informative is the approach used by Detwiler et al. (2000) with fracture analogs, which was also done at MIT. Figure 21 shows (a) cross-section through the MIT Hele Shaw cell with a transparent fracture analog; the transparent rough analog is shown in (b) and the principle of the tests in (c). The experiment consists of applying external stresses and fluid flow in the Hele Shaw cell such that fracture surfaces get increasingly deformed, and the flow (and transport) is affected as shown in (d). The effect of increasing normal stress is shown in more detail in Fig. 22.

Researchers have also constructed physical models to observe flow in jointed rock masses. Figure 23 shows aspects of what are probably the most ambitious and complex models in this domain, namely, those by Louis (1972). In these models the joints are represented by Plexiglas plates also including roughness. Given this complexity it is recommended to look at the original publication by Louis (1972). Not only shown but also well known are electrical resistor networks, which essentially are physical analogs.

Fig. 26 Base friction model. (**a**) Model equipment (Bray and Goodman 1981); (**b**) Schematic of base friction model by Egger (Bray and Goodman 1981). For results of the tests by Bray and Goodman (1981) see Fig. 30

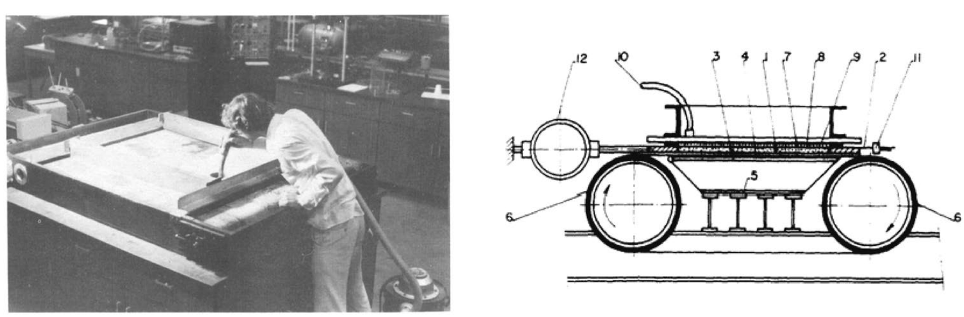

(a) (b)

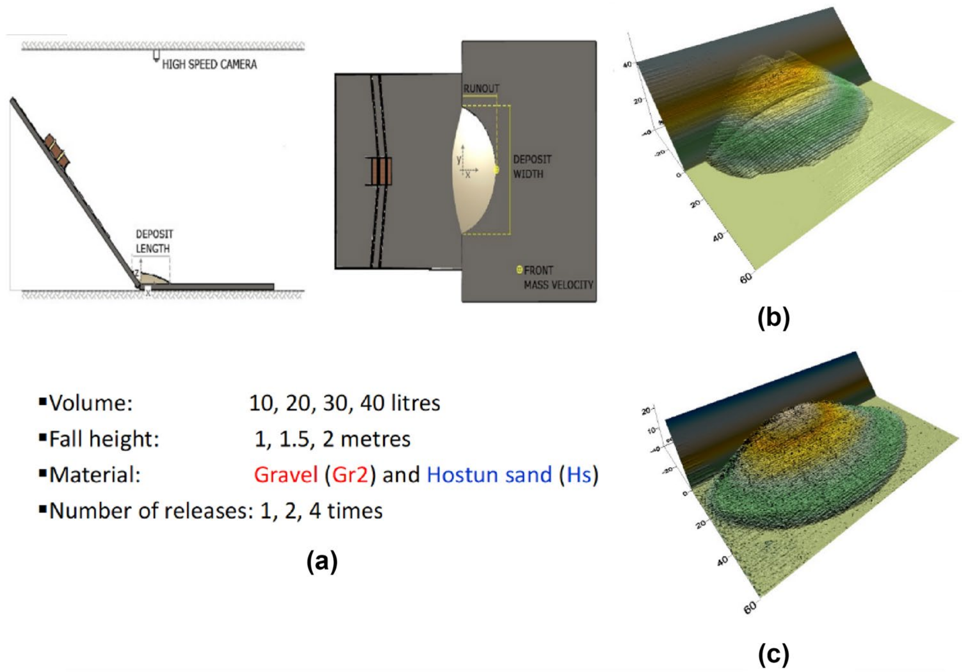

Fig. 27 Rock avalanche experiments by Manzella and Labiouse (2009). (**a**) Model setup; (**b**, **c**) Effect of different particle geometries, volumes, fall heights on resulting morphology of deposits

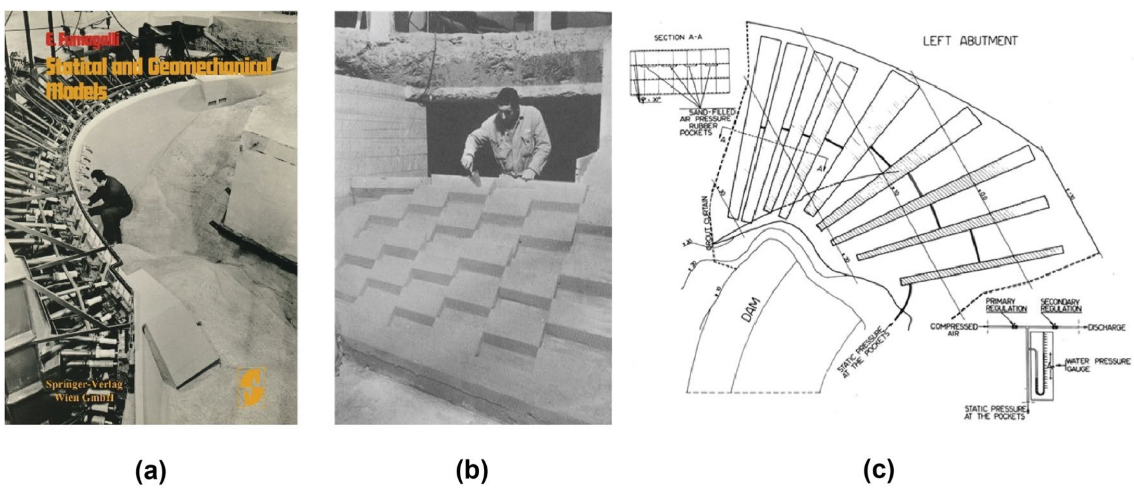

Fig. 28 Model of dam on jointed rock foundations (Fumagalli 1973). (**a**) Book cover "Statical and Geomechanical Models" showing dam and loading; (**b**) Jointed rock foundation; (**c**) Load application—in addition to external loads the pore pressure effects in the joints are modeled by air-pressurized bags in the joints

4 Complex Models

In this chapter physical models representing geologic mechanisms (tectonics, slope failure) and the interaction of structures and geology (Dams, Tunnels) will be discussed.

4.1 Physical Models of General Geologic Processes

Such models are further steps beyond the models of, e.g., Shelton (1912). Cloos (1930) used sheets of clay of different consistencies placed on a table as shown in Fig. 24a. By pushing a metal plate underlying the clay sheet different geologic mechanisms can be modeled and the resulting structures produced. Figure 24b shows not only a Graben produced by moving the underlying metal sheet in lateral extension but also the resulting faults. By including clay of different stiffnesses (more or less moist) it is possible to show different tectonic structures. Quite important are H. Cloos' initial comments on scaling in which, along the lines of Galilei, he states that true scaling of material properties

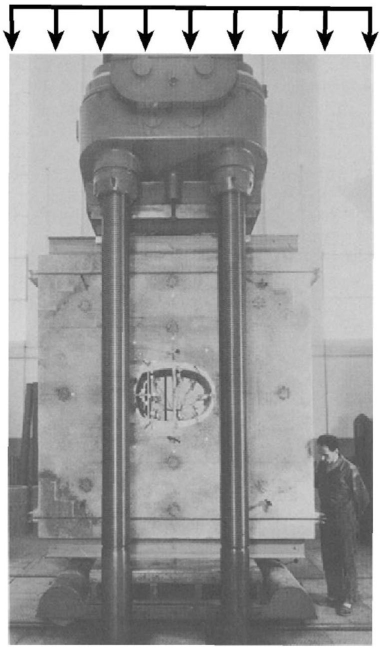

Fig. 29 ISMES model test on a lined tunnel under horizontal loading: setup is rotated by 90° (Fumagalli 1973). Arrows show load direction

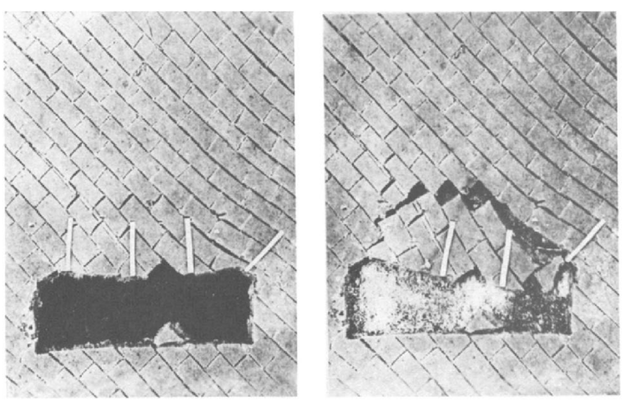

Fig. 30 Base friction test on a tunnel in jointed rock (Bray and Goodman 1981). (**a**) Condition before removing the bolt at the upper left; (**b**) Condition after removing the bolt at the upper left

is very difficult and that his models are to be understood as conceptual tools.

4.2 Physical Models of Jointed Slopes

Jointed rock slope models are probably the best-known physical rock engineering models mostly because of tests run by Müller in Karlsruhe on the rockslide at Mount Toc leading to the Vajont disaster (Fig. 25). In essence, the seat-shaped geometry underlying the jointed mass can facilitate a collapse of the blocky mass possibly producing a sudden pore pressure increase. One needs to know, however, that other interpretations of the Mount Toc failure exist (see, e.g., Hendron and Patton 1987).

Cloos' (1930) approach leads to the use of "base friction models" which go beyond conceptual models by introducing a way to consider the effect of gravity in the physical models. Modern base friction models as introduced by Bray and Goodman (1981) (Fig. 26) use a continually moving belt to produce the effect of gravity. As shown in this reference true scaling is now possible. Interestingly, Cundall et al. (1977) used a base friction model of a jointed rock slope to compare the modeling with the distinct element method.

The preceding, but considering in addition some movement during slope failures, logically leads to models of rock avalanches and rockfalls as were used, for instance, by Manzella and Labiouse (2009) (Fig. 27). A wide variety of parameters could be investigated with this model and then be compared to numeral models with good correspondence.

4.3 Physical Models of Structures on or in Rock

4.3.1 Models of Dams

Figure 28a shows the Book cover of "Statical and Geometrical Models" by Fumagalli (1973). This is shown for several reasons: The impressive dimensions and how the forces are applied are illustrated. ISMES led by Fumagalli was the center of the physical modelling effort, mostly for structures (bridges, buildings). The book goes into details of scaling. Regarding dams on rock there are several interesting aspects: very importantly, Fumagalli distinguishes between conventional and geomechanical models. In the former, aimed at performance of the dam per se, the foundation is a continuum consisting of properly scaled material. In the geomechanical model the behavior of the foundation is included and modeled by stacks of bricks (Fig. 28b). This includes different surfaces of the joints, hydrostatic loading of the dam by fluid-filled bags (fluid density varied for proper scaling), or hydraulic jacks as shown in Fig. 28c. A particularly interesting feature is the use of air pressure-filled bags in the joints making it possible to model varying pore/cleft water pressure (Fig. 28c).

4.3.2 Models of Tunnels

ISMES also used geomechanical models for tunnels (Fig. 29). This is, however, not quite correct since load is applied after the tunnel is built. The correct unloading mechanism can be applied in the base friction model as shown by Bray and Goodman (1981) (Fig. 30). As a matter of fact the base friction model correctly applies the effect of gravity,

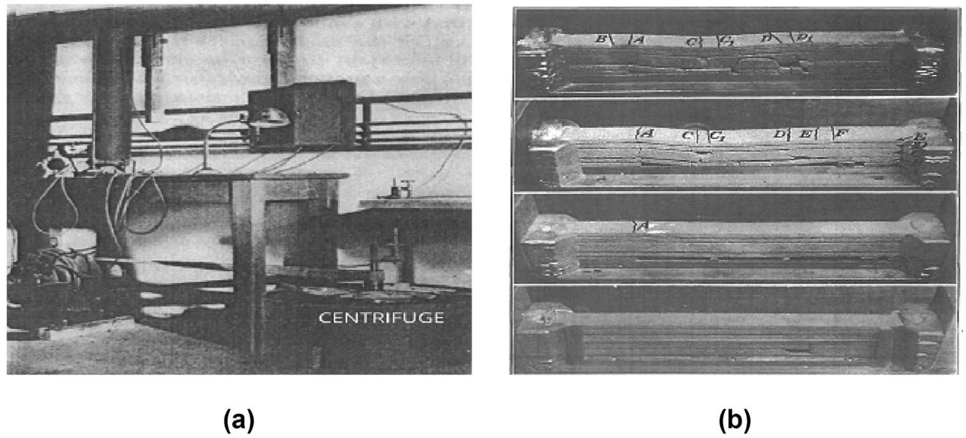

Fig. 31 Centrifuge test on a mine roof in layered rock (Bucky 1931). (**a**) Equipment setup; (**b**) results layer rock deforms more as load stresses increase from bottom to top. “A,” “B,” etc., indicate observed fractures caused by the deformation

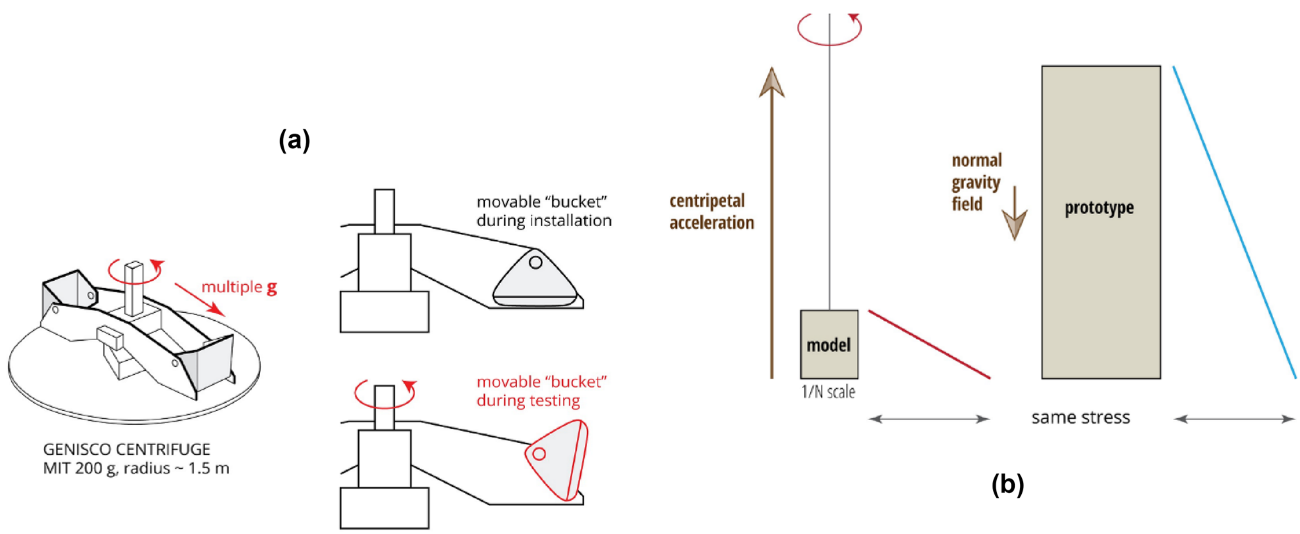

Fig. 32 Principle of stress scaling in centrifuge tests. (**a**) Genisco centrifuge—during rotation the centrifugal force applies multiple g in the horizontal direction; (**b**) Stress scaling

and scaling is to some extent possible with the choice of the friction coefficient between the moving belt and the two-dimensional model.

A step further in correct modeling of the in situ stress field is possible with the centrifuge. Bucky (1931) used the centrifuge for mining problems as shown in Fig. 31 where the roof deflections of an opening in layered rock were modeled. Figure 32 shows the principles of the stress modeling with the centrifuge.

Numerous centrifuge studies with tunnel models in soil have been conducted and will not be mentioned here. However, what will be mentioned is the limitation of using the centrifuge in jointed rock. While stresses and strains in a continuum can be properly scaled, displacements can to a limited extent only. Models of jointed rock can therefore be used conceptually (Fig. 33) but not in cases where, e.g., shearing resistance changing with displacement plays a role.

5 Physical Models in Rock Mechanics and Rock Engineering—Critical Aspects and Outlook

When discussing physical models, physical properties or laboratory experiments in general, the issue of scaling has to be addressed. As a matter of fact, this has been continuously addressed throughout this paper from Galilei to centrifuge modeling. Dimensional analysis (e.g., Lanhaar 1951) can be used to develop a proper model. Related to the specific issue of scaling in modelling jointed rock masses the reader is referred to Nelson (1968), who discusses in detail how the material for the model studies shown in Sect. 3.2 was selected. The process involved the selection of parameters that best represent the performance of the prototype, formulation of dimensionless products and variation of model material properties. Experiments had then to be conducted

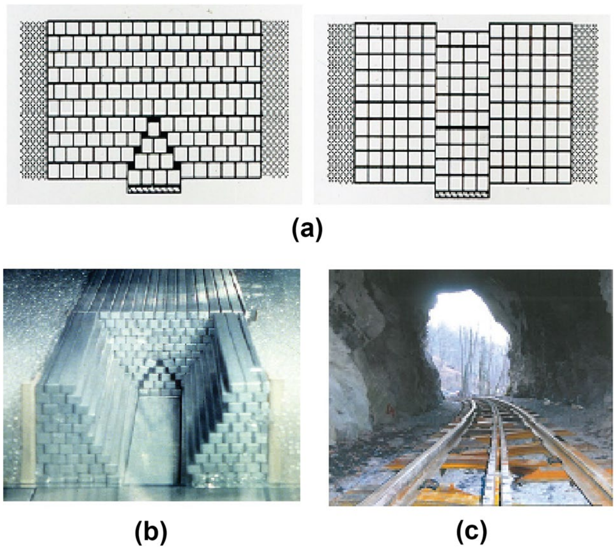

Fig. 33 Trapdoor test with the centrifuge on jointed rock. (**a**) Different rock block geometries; (**b**) Photo of displacement after test; (**c**) Real geometry that can be conceptually modeled as shown in (**b**)

to determine which material best satisfies the requirements. Such experiments, as any laboratory experiment, are subject to experimental scatter. These comments are made to show that although mathematically clear, the combination of mathematical complexity and experimental variability makes the selection of a model material not straightforward, and this is also so for other modeling conditions such as the geometry and the stress field.

If one compares such physical modeling to modeling with numerical simulation in which many parameters, many parameter states, and many external conditions can be simultaneously varied, the question comes up why use physical models at all. On the other hand, one has to mention the well-known questions and facts regarding simulation:

To what is the simulated performance compared?
The same simulated performance can be caused by a variety of unknown combinations of parameters, parameter states, and external conditions.

This leads to this final question: are neither the physical models nor simulations satisfactory?

The answer to this question may lie in many of the examples shown previously in this paper: Coulomb stipulated cohesion and proved it by physical model testing. The flow in a rough fracture subject to combinations of external stresses and internal pressure was simulated and then physically verified in the Hele-Shaw tests. Very often the verification process is reversed: Rock avalanches or shearing and tension in the persistence problem were tested and then simulated using the tested parameters.

In other words, and in conclusion, physical models are essential for verifying simulation models of specific mechanisms and simulation models can be used to expand parameter variation.

Acknowledgements The paper “Physical Modelling in Rock Mechanics and Rock Engineering” was presented both orally and in the proceedings of the 15th International Congress of the ISRM (Einstein, 2023) Extensive research on the topic with systematic work by the author was done and written up in a corresponding paper, which then was significantly shortened to adhere to the Congress requirements. Comments received by the author indicated that quite a few members of the rock mechanics and rock engineering community are interested in the detailed treatment of the topic. Hence, this extended version was develod. My students Omar AlDajani, Ignacio Arzuaga-Garcia and Randall Pietersen helped with the figures and proofreading.

Funding ’Open Access funding provided by the MIT Libraries’. No external funding was used.

Declarations

Conflict of interest The paper was prepared on MIT-time and there are no conflicting interests.

References

Addis B (ed) (2021) Physical models. Wilhelm Ernst & Sohn

Baecher GB, Lanney NA, Einstein HH (1977) Statistical description of rock properties and sampling. In: Proceedings of the 18th U.S. symposium on rock mechanics, pp 5C1–8

Barton N (1973) A review of a new shear strength criterion for rock joints. Eng Geol 7:287–332

Barton N, Bandis S (1982) Effects of block size on the shear behaviour of jointed rock. In: Keynote Lecture, 23rd US symposium on rock mechanics, Berkeley

Barton N, Choubey V (1977) The shear strength of rock joints in theory and practice. Rock Mech 10:1–65. https://doi.org/10.1007/BF01261801

Bobet A, Einstein HH (1998) Fracture coalescence in rock-type materials under uniaxial and biaxial compression. Int J Rock Mech Min Sci 35(7):863–889

Bray JW, Goodman RE (1981) The theory of base friction models. Int J Rock Mech Min Sci 18:453–468

Brown ET, Trollope D (1970) Strength of model of jointed rock. In: ASCE journal of the soil mechanics and foundation division, vol 96(SM2)

Bucky PB (1931) Use of models for the study of mining problems. Tch Publication No 425 AIMME 3-28

Call RD, Savely J, Nicholas DE (1976) Estimation of joint set characteristics from surface mapping data. In: Proceedings 17th U.S. symposium on rock mechanics, pp 2B2-1–2B2-9
Chan HCM, Li V, Einstein HH (1990) A hybridized displacement discontinuity and indirect boundary element method to model fracture propagation. Int J Fract 45(4):263–282. https://doi.org/10.1007/BF0003627
Chilton J (2021) Heinz Isler and his use of physical models. In: Addis B (ed) Physical models (Ch. 21). Wilhelm Ernst & Sohn
Cloos H (1930) Zur experimentellen tektonik—mechanik und beispiele. Die Naturwissenschaften 18(34)
Cloos E (1955) Experimental analysis of fracture patterns. Bul Geol Soc Am 66:241–256
Coulomb CA (1776) Essai sur une application des règles maximis at minimis à quelques problèmes de statique relatifs à L'architecture. Mémoires de Mathématique et Physique Présentés à l'Académie royale des Sciences par divers savans élûs dans ses Assemblées Vol 7 1773, Paris 1776. In J. Heyman (1972). Coulomb's memoir on statics, Cambridge University Press
Cundall P, Voegele M, Fairhurst C (1977) Computerized design of rock slopes using interactive graphics for the input and output of geometrical data. In: Proceedings 16th symposium on rock mechanics, pp 5–13
Dershowitz WS (1984) Rock joint systems (Doctoral dissertation). Massachusetts Institute of Technology, Department of Civil Engineering, Cambridge
Dershowitz WS, Einstein HH (1988) Characterizing rock joint geometry with joint system models. Rock Mech Rock Eng 21:21–51
Detwiler RL, Rajaram H, Glass RJ (2000) Solute transport in variable-aperture fractures: an investigation of the relative importance of Taylor dispersion and macro-dispersion. Water Resour Res 36(7):1611–1625
Einstein HH (2023) Physical modeling in rock mechanics and rock engineering. In: Schubert, Kluckner (eds) 15th ISRM congress 2023 & 72nd geomechanics colloquium. ÖGG
Einstein HH, Hirschfeld RC (1973) Model studies on mechanisms of jointed rock. ASCE J Geotech Div 99(3):229–248
Einstein HH, Hirschfeld RC, Nelson RA, Bruhn RW (1969) Model studies of jointed-rock behavior. In: Proceedings of the 11th U.S. symposium on rock mechanics (USRMS), 16–19 June, Berkeley, ARMA-69-0083
Einstein HH, Baecher GB, Veneziano D et al (1980) risk analysis for rock slopes in open pit mines—final technical report. Publication No. R80-17, Order No. 669 of joint set characteristics from surface mapping data. In: Proceedings 17th U.S. symposium on rock mechanics, 2B2-1–2B2-9
Einstein HH, Veneziano D, Baecher GB, O'Reilly KJ (1983) The effect of discontinuity persistence on rock slope stability. Int J Rock Mech Min Sci 20(5):227–236
Fumagalli E (1973) Statical and geomechanical models. Springer, Berlin
Galilei G (1638) Discorsi e dimostrazioni matematiche, intorno à due nuoue scienze
Goldstein M, Goosev B, Pyrogovsky N, Tulinov R, Turovskaya A (1966) Investigation of mechanical properties of cracked rock. In: 1st congress of the ISRM paper 3.49, vol 1, pp 521–524
Hayashi M (1966) Strength and dilatancy of brittle jointed rock masses—the extreme stochastics abs anisotropic failure mechanism. In: Proc. 1st congress of the IRM, Lisbon, vol 1, pp 295–302
Hendron AJ Jr, Patton FD (1987) The vaiont slide—a geotechnical analysis based on new geologic observations of the failure surface. Eng Geol 24:475–491
Hoek E (1968) Brittle failure of rock. In: Stagg KG, Zienkiewicz OC (eds) Rock mechanics in engineering practice. Wiley, London, pp 19–124
Hoek E, Carranza-Torres CB, Corkum B (2002) Hoek and Brown failure criterion 2002 edition. In: Proceedings of the North American rock mechanics society (NARMS)—Toronto, vol 1, pp 267–273
Isler H (1961) New shapes for shells. In: Bulletin of the international association for shell structures, Madrid, IASS, Paper C-3, No. 8
Iwano M, Einstein HH (1995) Laboratory experiments on geometric and hydromechanical characteristics of three different fractures in granodiorite. In: Proceedings of the 8th ISRM congress, 25–29 September, Tokyo, ISRM-8CONGRESS-1995-151
Kienast H (2005) 2005, The aqueduct of Eupalinos on Samos. Archaeological Receipts Fund, Directorate of Publications, Athens
Ladanyi B, Archambault G (1969) Simulation of shear behavior of a jointed rock mass. In: Proceedings of the 11th U.S. symposium on rock mechanics (USRMS), 16–19 June, Berkeley
Lanhaar HL (1951) Dimensional analysis and theory of models. Wiley, New York
Louis CL (1972) Rock hydraulics. In: Müller L (ed) Rock mechanics, courses and lectures no 165. Springer, pp 93–109
Manzella I, Labiouse V (2009). Flow experiments with gravel and blocks at small scale to investigate parameters and mechanisms involved
Mindrup M (2019) The architectural model: histories of the miniature and the prototype, the exemplar and the muse. The MIT Press, Cambridge
Mohr O (1906) Abhandlungen aus dem Gebiet der technischen mechanik. W. Ernst & Sohn, Berlin
Müller L (1980) Sinn und Berechtigung von Modellversuchen in der Geomechanik Forschung. Rock Mech 13:39–52
Nelson RA (1968) Modeling a jointed rock mass. MIT MSc Thesis
Nelson JW (1977) Shear resistance of discontinuities in rock. MIT MSc Thesis
Patton FD (1966) Multiple modes of shear failure in rock. In: Proceedings of the 1st congress of the international society of rock mechanics, pp 509–513
Reyes O, Einstein HH (1991) Failure mechanisms of fractured rock—a fracture coalescence model. In: Proceedings of the 7th ISRM congress, 16–20 September, Aachen, pp ISRM-7CONGRESS-1991-066
Riedel W (1929) Zur Mechanik geologischer Brucherscheinungen. Zentralblatt für Mineralogie Abt B, pp 354–368
Rosenblad L (1969) Development of equipment for testing models of jointed-rock masses. In: Proc.11th U.S. symposium on rock mechanics (USRMS), Berkeley, June 1969. Paper Number: ARMA-69-0127
Rosengren KJ, Jaeger JC (1968) The mechanical properties of an interlocked low-porosity aggregate. Géotechnique 18(3):317–326
Shelton P (1912) Some observations and experiments on joint planes. J Geol 20(2):164–183
Barton NR (1970) A model study of the behaviour of steep excavated slopes. PhD Thesis Univ. of London
Barton NR (1971) A relationship between joint roughness and joint shear strength. Symp. Soc. Internatl. Mécanique des Roches, Nancy